Test of a Steel Plate Shear Wall with Partially Encased Composite Columns and RBS Frame Connections

Mehdi Dastfan, A.M.ASCE[1]; and Robert Driver, M.ASCE[2]

Abstract: A large-scale steel plate shear wall with partially encased composite (PEC) columns and reduced beam section (RBS) frame connections was tested at the University of Alberta to investigate the behavior of the system and quantify some key characteristics related to seismic design of this system. The use of RBS connections was intended to reduce the demand on the beam-to-column connection and obtain improved seismic performance. Subjected to quasi-static cyclic load until severe damage was observed, the specimen showed desirable characteristics such as high elastic lateral stiffness, ductility, and energy dissipation capacity. The use of RBS frame connections was proven to be a viable option to improve the seismic performance of these walls. The test observations indicated that the detailing of the PEC columns played an important role in improving the seismic performance of the specimen. Several design and detailing recommendations have been made based on the observations during this test and previous experimental studies. **DOI: 10.1061/(ASCE)ST.1943-541X.0001954.** © *2017 American Society of Civil Engineers.*

Author keywords: Steel plate shear wall; Reduced beam section (RBS) frame connection; Partially encased composite column; Quasi-static cyclic test; Ductility; Energy dissipation; Elastic lateral stiffness; Seismic detailing; Metal and composite structures.

Introduction

Steel plate shear walls are a well-known system for bracing structures against lateral loads such as wind or earthquake. They consist of a thin steel infill plate inside a surrounding frame of beams and columns. The strength and stiffness of this system is highly dependent on the post-buckling capacity of the infill plate (i.e., tension field action). To develop an efficient and fairly uniform tension field in the infill plate for effective seismic performance, adequate flexural stiffness of the columns and beams in the surrounding frame must be provided. In addition to the forces introduced into the columns due to anchorage of the tension field in the infill plate (compression in one column and tension in the other), the columns also carry the gravity forces introduced by dead and live loads. Dastfan and Driver (2008, 2009) studied the flexural stiffness requirements for the columns and the beam at the top of steel plate shear walls, as well as the effect of the frame connection rigidity on these requirements. The Canadian steel design standard [CSA S16-14 (CSA 2014)] and the AISC seismic provisions for structural steel buildings [ANSI/AISC 341-10 (AISC 2010)] specify the minimum flexural stiffness requirements for frame elements surrounding the infill plates. These demanding stiffness requirements make the composite column a viable option for steel plate shear wall systems.

In order to facilitate construction and reduce overall in-place cost primarily in high-rise buildings, the Canam Group introduced partially encased composite (PEC) columns (Vincent and Tremblay 2001). PEC columns consist of three relatively thin plates that form an H-shaped steel section. Transverse links are welded near the tips of the two flanges with an appropriate spacing to increase their local buckling strength. Use of the same plate thickness for the web and flanges, fast skeleton erection, and the use of lighter cranes and simple formwork are some of the advantages of this type of composite column.

Since 1998, several experimental and numerical studies on the behavior of the PEC column as a single axially loaded member have been conducted. The effect of flange slenderness, link spacing, and longitudinal and extra transverse reinforcement (Tremblay et al. 1998; Chicoine et al. 2002b), as well as the effect of concrete confinement and residual stresses and imperfections in the flanges (Chicoine et al. 2002a), on the behavior of the column were studied. The behavior of the column under combined axial load and bending moment was experimentally studied, and axial load-bending moment (P-M) interaction diagrams were produced and verified (Bouchereau and Toupin 2003; Prickett and Driver 2006). Begum et al. (2007) conducted several parametric studies that were used to evaluate the design equations for PEC columns in the Canadian steel design standard, CSA S16-14.

Tremblay et al. (2003) conducted a numerical seismic/dynamic analysis to study the behavior of PEC columns as gravity columns, as well as the bracing bent columns in a concentrically braced steel frame. The behavior of PEC columns as part of a steel plate shear wall was investigated numerically and experimentally at the University of Alberta (Deng and Driver 2007; Deng et al. 2008). The large-scale steel plate shear wall test specimen in that study, called hereafter the benchmark test, had two stories and one bay, and the surrounding frame had rigid connections. Under quasi-static cyclic loading, according to the provisions of ATC-24 (ATC 1992), the specimen exhibited a yield displacement of 7 mm (yield story drift of 0.37%) and a peak base shear of 1,817 kN (30% larger than yield base shear) with a corresponding first-story deflection of 35 mm (story drift of 1.84%). The test was terminated because of significant column flange and web tearing, accompanied by severe concrete crushing and failure of a few links in the column plastic hinge locations. One main observation in the benchmark test was the formation of partial plastic hinges at the top and bottom

[1]Senior Bridge Engineer, COWI North America Ltd., Edmonton, AB, Canada T6G 2C8 (corresponding author). E-mail: medn@cowi.com

[2]Professor, Dept. of Civil and Environmental Engineering, Univ. of Alberta, Edmonton, AB, Canada T6G 1H9. E-mail: rdriver@ualberta.ca

Note. This manuscript was submitted on February 26, 2017; approved on July 21, 2017; published online on November 17, 2017. Discussion period open until April 17, 2018; separate discussions must be submitted for individual papers. This paper is part of the ***Journal of Structural Engineering***, © ASCE, ISSN 0733-9445.

of the columns in the first story, initiating the formation of a soft story failure mechanism and causing a significant strength reduction. A modular steel plate shear wall specimen with PEC columns was tested by Dastfan and Driver (2016). The size of the beams and columns were similar to the benchmark test and the infill plates had the same thickness; however, the detailing was different. The frames had bolted shear connections, and the infill plates were bolted to fish plates welded to the frame members. All bolts were pretensioned. Longitudinal rebars at the base of the columns were added to improve the behavior of the plastic hinge region. The link spacing was also reduced in this region for higher local buckling capacity of the column flanges, as well as better concrete confinement. All these improvements in the hinge region increased the ductility of the system. The modular steel plate shear wall specimen exhibited a yield displacement of 10 mm (yield story drift of 0.53%) and a peak base shear of 1,821 kN (30% larger than yield base shear) with a corresponding first-story deflection of 42.5 mm (story drift of 2.24%). The modular construction method did not appear to have any negative effect on the overall behavior of the system and provided high lateral stiffness in the elastic range and desirable seismic characteristics in the postyield stage. Although by the end of the test several regions of the infill plate had torn and complete tearing of the outer flanges of the columns was observed, there was no sudden decrease in the overall strength of the specimen.

To further investigate the behavior of steel plate shear walls with PEC columns, a wall specimen with PEC columns and reduced beam section (RBS) frame connections, hereafter called the RBS test specimen, was designed similarly to the modular test specimen and tested at the University of Alberta. The objective of this test was to gain an understanding of the effect of RBS connections on the seismic performance of the wall systems with PEC columns. Similar to most of the post-Northridge connection designs, RBS connections are intended to move the plastic hinge location away from the column face and reduce the demand on the beam-to-column connection. This is achieved by weakening the beam section away from the column face by removing portions of its flanges (Moore et al. 1999). It has been shown that the effect of RBS connections on the elastic lateral stiffness of frames is small: a 50% reduction in the flange width reduces the frame stiffness only 5–7% (Grubbs 1997). As a result, similar to the bolted shear connections in the modular test specimen (Dastfan and Driver 2016), the RBS connections should not alter the stiffness of the specimen in the elastic range significantly. However, by developing plastic hinges in the reduced section at the postyield stage, this type of connection should reduce the stress at the beam-to-column connection and postpone the initiation of the formation of soft stories.

Test Specimen, Test Setup, and Instrumentation

The RBS test specimen was a two-story steel plate shear wall with a modified beam-to-column connection. In order to achieve better performance compared to the benchmark test and postpone the initiation of the soft story mechanism, RBS connections with radius cuts were selected to be used in the beam-to-column connections at both ends of the intermediate beam. The cross section of the top beam was not reduced because based on the Canadian steel design standard, CSA S16-14, plastic hinges are permitted to form at the tops of columns instead of in the beams at the roof level. In the case of the RBS test specimen, even the deepest-cut RBS at the top level would not prevent a hinge from forming in the adjacent PEC columns because of the large depth of the beam.

The RBS test specimen had the same overall height (4,120 mm) and width (2,690 mm) as the modular one. The story heights were 1,900 mm, and the columns had a center-to-center distance of 2,440 mm. The PEC columns had a 250 × 250 mm cross section. The flanges and web of the columns had a thickness of 6.35 mm, and the infill plate thickness was 3.0 mm in both stories. Like the modular test specimen, PEC columns in the RBS specimen conformed to the requirements of the Canadian steel design standard, CSA S16-14, regarding the minimum moment of inertia. The links were 10-mm-diameter smooth bars and were placed at a closer spacing at the base of the columns ($s/b = 0.2$, where s is the link spacing and b is the column flange width) and close to the frame connections ($s/b = 0.32$), where a higher rotational ductility was required to postpone the buckling of the flanges and increase the ductility of the section by providing some confinement to the concrete. In order to postpone the crushing of concrete within the plastic hinges at the base of the columns and to reduce the strength degradation of the steel portion of the columns due to damage close to the end of the test, 750-mm-long 25M longitudinal rebars were installed. Fig. 1 shows the cross section of the PEC column. Fig. 2 depicts the elevation view of the RBS test specimen.

The RBS cuts were circular and the cut dimension and location were selected based on the suggestions by Moore et al. (1999). Fig. 3 depicts the plan view of the RBS cuts at the first-story frame connections. The surfaces of the cuts in the RBS region were ground smooth to remove any notches and avoid fracture or low cycle fatigue failure in the cut portion. 12.7-mm-thick side plates were welded to the tips of the flanges of the columns in the frame connection locations to increase the stiffness and strength of the column flanges, and filler plates were welded between the side plates and the top and bottom beam flanges.

The infill plate and column plates had static yield stresses of 260 and 448 MPa, respectively. The flanges of the first- and second-story beams had static yield stresses of 352 and 356 MPa, respectively, whereas for the webs the yield stresses were 380 and 360 MPa, respectively. The static yield stresses of the 25M longitudinal rebars and links were 447 and 405 MPa, respectively. The 28-day compressive strengths of the concrete in the columns of the first and second stories were 49 and 44 MPa, respectively.

The elevation of the test setup is shown in Fig. 4. The test specimen was connected to the strong floor by 12 high-strength pretensioned anchor rods. The out-of-plane displacement of columns was prevented at each floor level by articulated braces. To represent the service gravity loads, constant vertical forces of 600 kN were applied to the tops of the columns, which is about 20% of their axial capacity. The gravity loads were applied through a cross-shaped distributing beam that was connected to actuators mounted on four gravity load simulators installed at the base of the wall. The quasi-static lateral loads were applied by two sets of actuators, which were supported by a reaction wall, directly to the top flanges of the floor beams. Equal lateral loads were applied to each floor

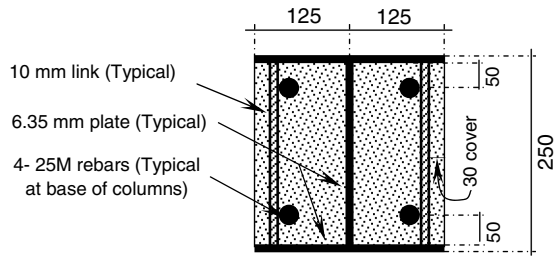

Fig. 1. Cross section of PEC column

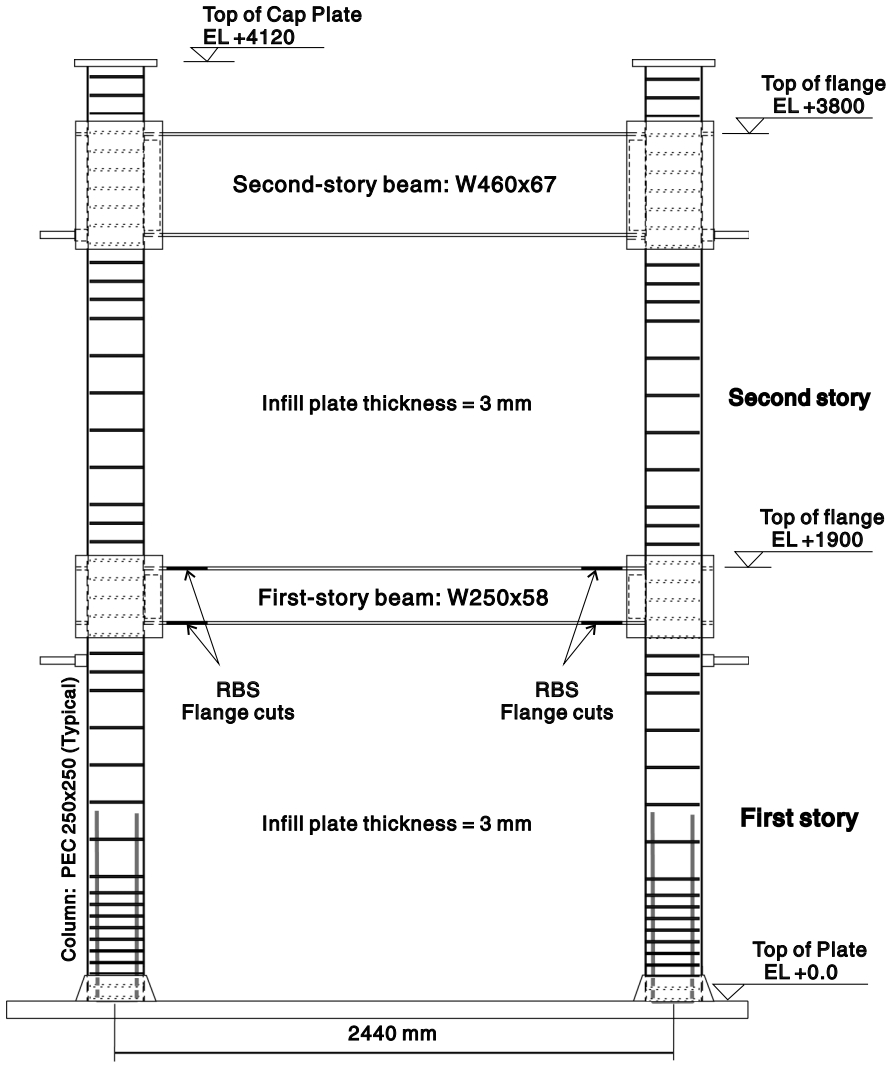

Fig. 2. Elevation view of the RBS steel plate shear wall test specimen

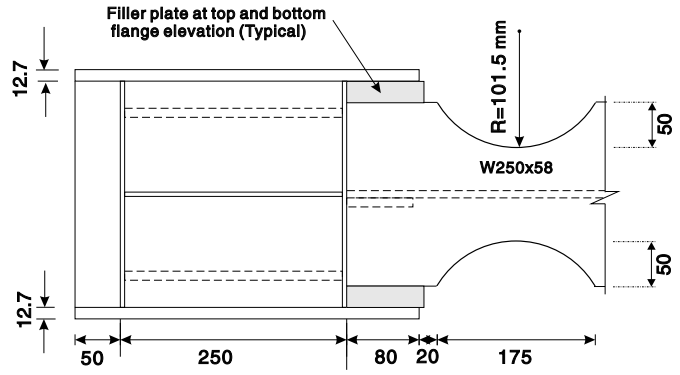

Fig. 3. Plan view of the RBS cuts at the first-story frame connections

because the focus of this test was the behavior of the first story and the applied load to the second-story beam was to have the infill plate of the second story buckle and enter the post-buckling stage.

The lateral loading regime was based on the method outlined in ATC-24. For the *force control* stage, the base shear (Q) was selected as the controlling parameter and the first-story deflection (δ) was chosen as the controlling parameter in the *displacement control* stage. Q_y, the yield value of force control parameter, was estimated to be close to that of the benchmark test, i.e., 1,400 kN. The value of δ_y, the yield value of the displacement control parameter, was chosen as 10 mm. Table 1 shows the target controlling parameters in different loading cycles of the test.

The rotations of the frame connections were measured by clinometers. The first-story beam-to-column connection rotation was measured by two clinometers, one measuring the rotation of the column side plate and the other measuring the beam rotation at the end of the RBS cut toward the center of the beam. The in-plane floor displacements were measured by cable transducers. The movement of the base plate was also monitored during the test to adjust the story deflections had the base plate moved, but measurements showed that its movement was negligible. The strains in the infill plates, column flanges, longitudinal rebars at the base of the columns, and one of the RBS cuts were measured by electrical resistance strain gauges and strain gauge rosettes. A total of 111 channels of data were recorded during the test.

Two three-dimensional (3D) camera systems were used to monitor the strains at the base of the north column during the test. The monitored areas were the outer flange and the side face of the column, which were the steel and concrete faces, respectively.

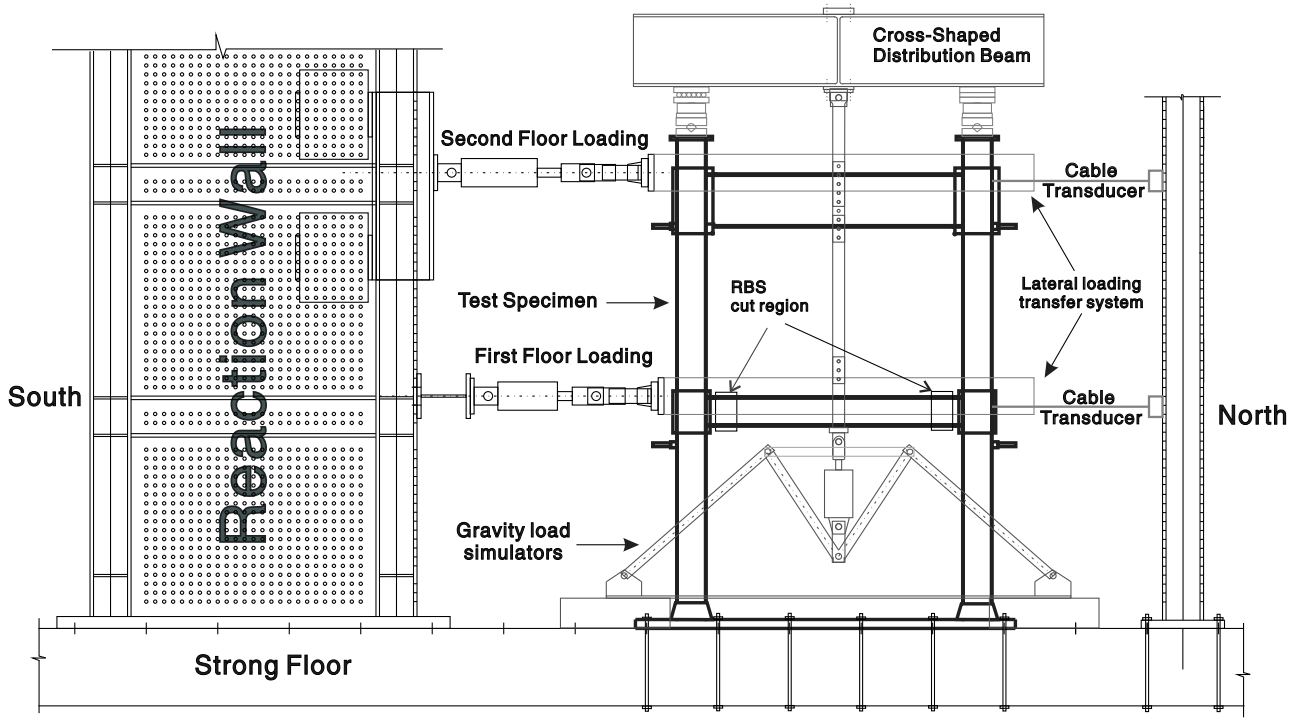

Fig. 4. Elevation of test setup

Table 1. Target Controlling Parameters in Different Cycles of the Test

Cycle number	Force control parameter, Q, base shear (kN)	Displacement control parameter, δ, first-story deflection (mm)	Drift demand in first story (%)
1–3	±350	—	—
4–6	±700	—	—
7–9	±1,050	—	—
10–12	—	$\delta y = \pm 10$	±0.53
13–15	—	$2\delta y = \pm 20$	±1.05
16–18	—	$3\delta y = \pm 30$	±1.58
19–20	—	$4\delta y = \pm 40$	±2.11
21–22	—	$5\delta y = \pm 50$	±2.63
23–24	—	$6\delta y = \pm 60$	±3.16
25–26	—	$7\delta y = \pm 70$	±3.68
27	—	$8\delta y = \pm 80$	±4.21

Test Observations and Results

The application of the gravity load did not cause any local buckling of the column flanges, or cracking or crushing of the concrete, which was indicative of relatively concentric load application and elastic behavior of the columns.

During the nine force control cycles, shear buckling of the infill plates was evident in both stories and as the test progressed, the number of buckle waves increased. Several loud noises were heard during the load reversal because of the reorientation and popping through of the buckle waves. These noises were heard in all subsequent cycles. Diagonal cracks in the concrete close to the base of the columns indicated high shear forces at those locations. The presence of some horizontal cracks at the top of the columns in the first story indicated that the columns were deforming in double curvature. The cut region of the RBS connection did not show any sign of yielding, and no local buckling was detected in the flanges of the PEC columns.

During Cycles 10–12, i.e., the first displacement control cycles, the whitewash on parts of the infill plate of the first story started to flake off, showing a sign of yielding. The diagonal cracks close to the base of the columns propagated, and new cracks developed parallel to the existing cracks. In Cycles 13–15, the whitewash on the outer flanges of the columns at the base and the bottom flange and web of the first-story beam in the RBS cut region started to flake, which was an indication of yielding. Because the base of the columns, the RBS cut regions, and the infill plate of the first story were considered the critical regions of the test specimen, designated as protected zones or fuses in the Canadian and American steel design standards (CSA 2014; AISC 2010), it was concluded that significant yielding happened during this cycle in the intended zones.

Propagation of diagonal cracks in the concrete close to the base of the columns and local concrete crushing just above the side plates occurred in Cycles 16–18. The outer column flanges started to tear at the base of the columns and buckled at the midheight of the first story, about where the longitudinal 25M bars were terminated and the link spacing was largest. The infill plate in the first story started to tear from the welding access hole in the top south corner. In Cycles 19 and 20, in the compression region at the base of the columns just above the side plates, the diagonal cracks in the concrete further propagated and crushing of concrete was evident. The maximum base shear of 1,890 kN (35% larger than the yield base shear) was attained in Cycle 19.

During Cycles 21 and 22, the infill plate of the first story started to tear diagonally close to the north bottom corner. The outer flanges of the columns at the bases tore completely, causing only an 8% reduction in the base shear capacity. A new diagonal crack was detected in the top portion of the north column, indicating the presence of a high shear force in the columns in the region with the largest link spacing. The crushed concrete zone at the base of the columns extended slightly upward during these cycles. In Cycles 23 and 24, propagation of the column flange tearing to the web was detected and the length of the web tears was estimated

Fig. 5. Base of south column and adjacent infill plate at end of test

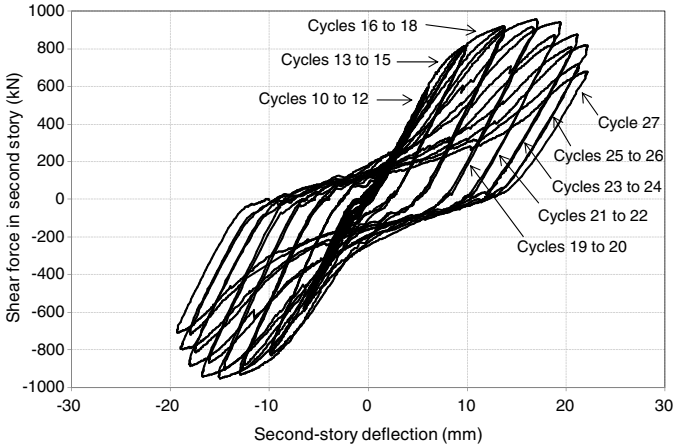

Fig. 7. Shear force in second story versus second-story deflection

to be approximately 30 mm. The infill plate in the first story suddenly tore more than 300 mm in the vertical direction close to the midheight of the story and adjacent to the connecting weld to the south column. Despite the partial separation of the infill plate from the column, the base shear capacity was reduced by only another 8%. There was evidence of development of a plastic hinge at the top of the columns in the first story, which is attributed to a redistribution of the bending moment to the top because of the severe crushing of concrete resulting in moment capacity degradation at the base.

In Cycle 25, the length of the vertical tear in the infill plate adjacent to the south column reached 800 mm, which caused a reduction in the number of buckle waves in the infill plate in the first story. The buckle waves were concentrated in the half of the infill plate anchored to the north column. The inner flange of the south column buckled as a result of the extra demand on the column due to the vertical tear of the infill plate adjacent to this column. The outer flanges of the north column buckled under the side plate of the first-story frame connection, which indicated the formation of a hinge. During Cycle 26, the vertical tear in the infill plate reached the base plate and, practically, the infill plate was no longer connected to the south column in the first story. The infill plate in the first story also started to tear diagonally from the top corners in the north and south, where the weld access holes were located. Plastic hinges were clearly evident at the tops of the columns in the first story.

The test was terminated after Cycle 27 because the base shear decreased to 75% of the peak base shear and there was serious damage in the columns and the infill plate of the first story. Fig. 5 shows the base of the south column and the adjacent infill plate at the end of the test. The yield lines and the vertical tear of the infill plate can be seen in this figure, in addition to the column damage.

The hysteretic loops of the first and second stories are shown in Figs. 6 and 7, respectively. As can be seen in these figures, the specimen showed a very high initial lateral stiffness and behaved elastically, before significant yielding of steel as well as tearing of the infill plate and further cracking of concrete began in Cycle 13. In Fig. 8, the hysteretic loops (base shear versus first-story deflection curves) resulting from Cycles 17 ($\delta = 3\delta y = 30$ mm) and 27 ($\delta = 8\delta y = 80$ mm) are shown for comparison. Similar to the hysteretic loops of previous tests on unstiffened steel shear panels, the hysteretic loops are pinched in the middle as a result of buckling wave reorientation, during which the majority of the stiffness is provided by the frame. The slope of the pinched part of the curve (i.e., Segments a-b and a′-b′) in Cycles 17 and 27 are 30 and

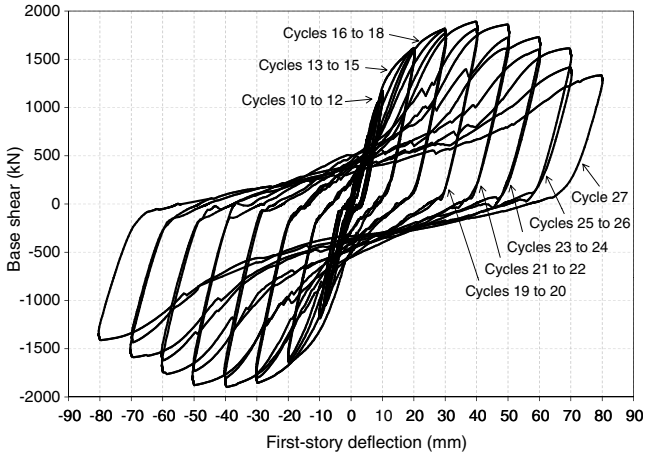

Fig. 6. Base shear versus first-story deflection

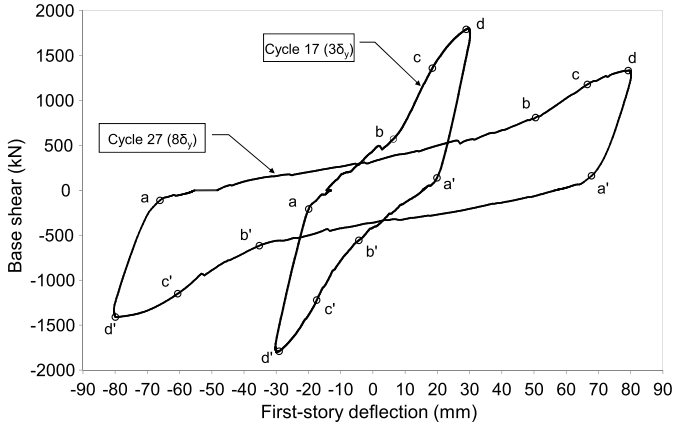

Fig. 8. Hysteretic loops of Cycles 17 and 27

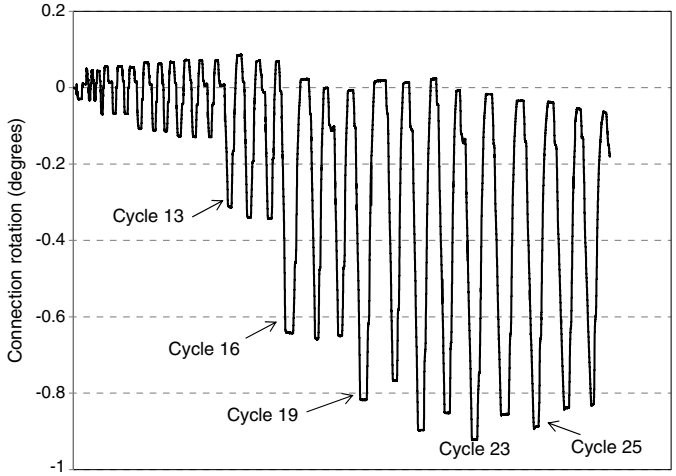

Fig. 9. Rotation history of RBS connection at north end of first-story beam

7 kN/mm, respectively. The slope of the Segment b-c, during which the tension field redevelops and causes the stiffness to increase, are 70 and 23 kN/mm in Cycles 17 and 27, respectively. Most of the damage, including the tearing and yielding of steel as well as cracking of the concrete, happened during Segment c-d because the base shear approached its maximum value in these cycles. The damage in this part caused a gradual decrease in the stiffness of the specimen. The lateral load was removed during Segment d-a′. The slope of this part of the curve was 163 kN/mm in Cycle 17 and 105 kN/mm in Cycle 27. Curve a′-b′-c′-d′-a represents reloading and unloading in the opposite direction, and the same behavior repeats.

Fig. 9 shows the rotation history of the RBS connection in the first story at the north end of the beam, defined as the relative rotations of the two adjacent clinometers, with the majority of these deformations taking place within the RBS region. The maximum rotation of the connection was approximately 0.9°. The RBS connection started to deform because of undergoing plasticity in Cycle 13, during which the connection rotation was almost twice that of Cycle 12. The maximum rotation in the first-story frame connection happened in Cycle 23. Because of the eventual formation of the plastic hinges at the tops of the first-story columns under the side plates, the beam-to-column connection rotation decreased slightly in Cycle 25. It is noted that the mean rotation shown in Fig. 9 tended to migrate gradually in one direction. This phenomenon is because the bending moment and the resulting rotation in column changes the direction between the two halves of each cycle, whereas the rotation of the end of the beam is always in one direction because of the first-story infill plate pulling down on the beam.

The data collected from the strain gauges at the column base and strain gauge rosettes on the infill plate of the first story showed complete yielding of the outer column flanges and uniform yielding of the entire infill plate in Cycle 13. Also, the strain readings from the RBS cut region indicated that the bottom flange and part of the web of the beam in the first story yielded in the first half of Cycle 13. This is attributed to the addition of the compression stresses due to bending and the axial compressive force in the first-story beam that was developed to anchor the tension field in the infill plates. Full cross-sectional yielding of the RBS connection was observed in Cycle 16.

Another observation in the RBS cut section was that the strains were bigger at the quarter point of the cut closer to the column than in the middle of the cut, which is the location of the smallest flange width. A similar observation was made by Qu and Bruneau (2010) in a test of a steel plate shear wall with RBS connections and conventional steel columns.

Fig. 10 shows the out-of-flatness deformations and the vertical strain distribution in the outer flange of the north column at the base in Cycle 18. These contours were produced by the 3D camera system. As can be seen in this figure, the flange buckled above the side plate as well as between the side plates at the base. The maximum vertical strain at the crest of the buckle waves in the same cycle was around 4%, which is higher than the strain-hardening strain. The path of the tear in the flanges of the column at the base, which started in Cycle 17, was through the crest of the buckle wave between the side plates. This observation indicates that the reason for the tearing in this area was low-cycle fatigue of the steel due to several cycles of folding and unfolding in that region.

To study the behavior of the concrete in the columns at the expected hinge location close to the base, the west side of the north column was monitored by another set of cameras. Fig. 11 shows the principal strain distribution in Cycles 13 and 21. The concrete started to crack on the tension side, adjacent to the inner flange, during Cycle 13. The crushing of the concrete on the compression side close to the base of the column initiated in Cycle 19 by development of vertical cracks in the compression zone, which extended through Cycle 21.

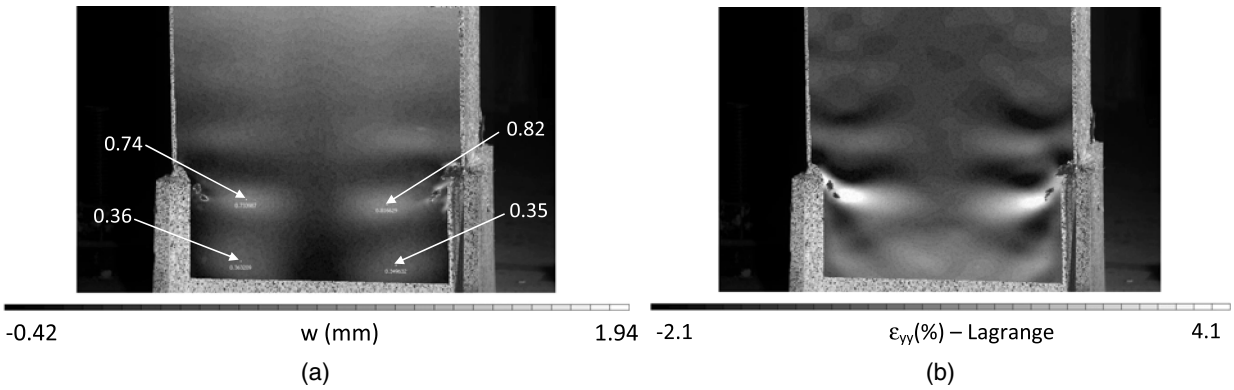

Fig. 10. Outer flange at base of north column in Cycle 18: (a) out-of-flatness deformation; (b) vertical strain distribution

J. Struct. Eng., 2018, 144(2): 04017187

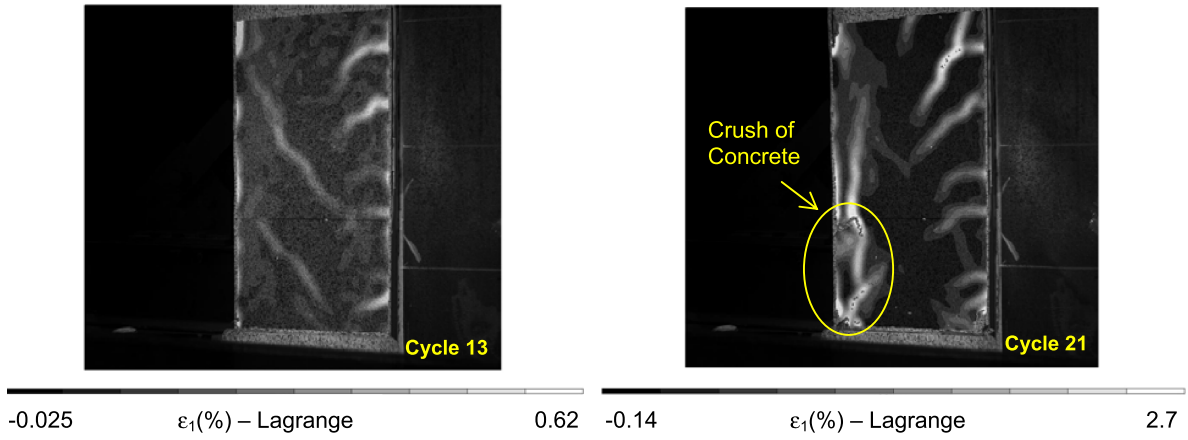

Fig. 11. Maximum principal strain distribution in concrete at base of north column in Cycles 13 and 21

Evaluation of Test Results

Lateral Stiffness and Displacement Ductility

High elastic stiffness of a lateral load resisting system is an important characteristic to minimize story drifts under service loads. During a severe earthquake, the system needs to absorb and dissipate energy by accommodating nonlinear deformation without strength degradation. For comparative evaluation of the lateral stiffness and displacement ductility, the envelopes of the base shear versus first-story deflection (in the positive region) for the benchmark, modular, and RBS specimens are shown in Fig. 12. The lateral stiffness of the first story of the RBS specimen in the elastic phase (i.e., before Cycle 13) was 140 kN/mm, as compared to 180 kN/mm for the benchmark and modular specimens. Although, because of the shape of the initial imperfection of the infill plate, the value for the RBS system is slightly lower, it is still a very stiff system. The envelope curves in Fig. 10 show that the overall behavior of the RBS specimen is similar to that of the modular one, and the improved column detailing of these systems over that of the benchmark case influenced mainly the postpeak performance.

Based on the test data, the yield deformation of the specimen and associated base shear were confirmed as $\delta_y = 10$ mm and $Q_y = 1{,}400$ kN, respectively. The displacement ductility, μ, of the specimen, as the ratio of the first-story deformation, δ, to the yield deformation, δ_y, was calculated at the peak base shear (in Cycle 19) and at 90% of the peak base shear in the postpeak phase (in Cycle 23). The corresponding displacement ductilities were $\mu = 4.0$ and $\mu = 6.2$, respectively. These values are approximately 95% of those obtained for the modular test specimen (Dastfan and Driver 2016).

Energy Dissipation Capacity

The energy dissipation in the specimen is mainly from yielding and tearing of steel and cracking and crushing of concrete. In order to evaluate the energy dissipation capacity of the specimen, the enclosed areas of the hysteretic loops (Figs. 6 and 7) are calculated in each cycle, as an indication of the amount of dissipated energy, and plotted in Fig. 13 for comparison. It can be seen that the amount of dissipated energy in the first story had two sudden increases, in Cycles 7 and 13, similar to the modular specimen (Dastfan and Driver 2016). During Cycle 7, the first yielding took place in some parts of the infill plate in the first story, and in Cycle 13, parts of the RBS cut regions at the ends of the first-story beam yielded and a partial plastic hinge formed there, resulting in yielding of all parts of the infill plate in the first story. The amount of dissipated energy in the second story was negligible up to Cycle 13, in which the frame connections of the first story started to rotate and, as a result,

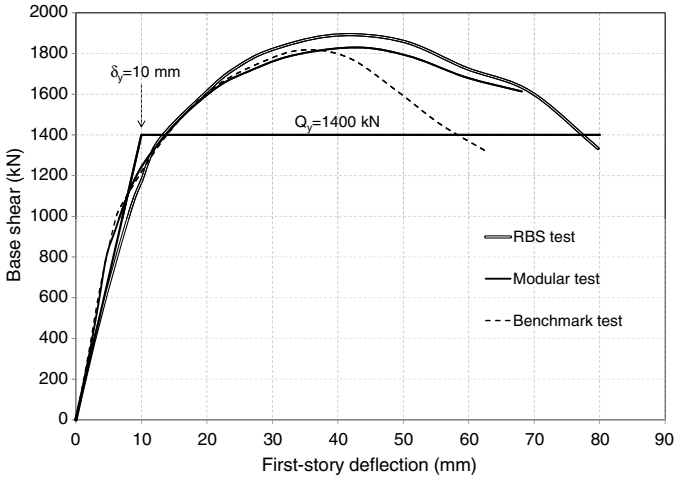

Fig. 12. Envelopes of base shear versus first-story deflection

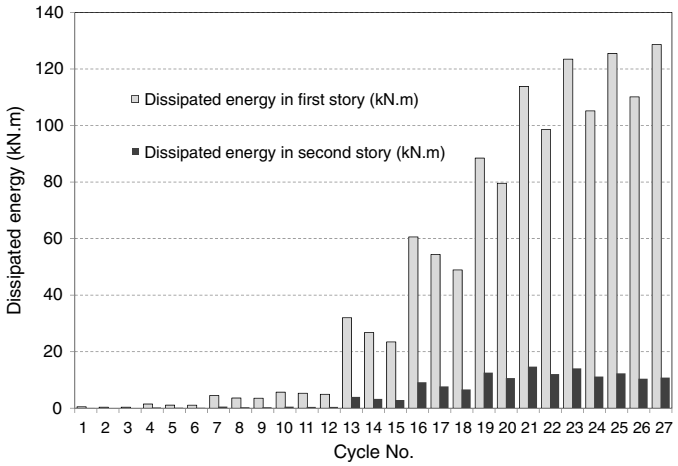

Fig. 13. Dissipated energy in first and second stories

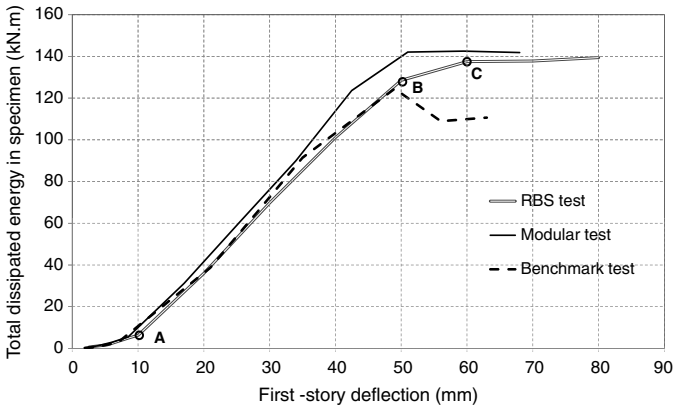

Fig. 14. Total dissipated energy per cycle versus first-story deflection

parts of the infill plate in the second story yielded. Most of the damage happened in the first cycle of each stage of displacement, so the amount of dissipated energy in the first cycle of each stage was larger than in subsequent cycles to the same displacement.

In Fig. 14, the total dissipated energy per cycle for the benchmark, modular, and RBS tests is plotted versus the first-story deflection. At Point A, which represents the cycle during which the RBS specimen reached its yield displacement, the slope of the curve increases suddenly because of the significant yielding in the infill plates and the frame connections in the first story. The slope decreases at Point B mainly because of the tearing of the outer flanges of the columns at the base. The further decrease at Point C is due to the vertical tear in the infill plate of the first story, which completely detached the infill plate from the south column. As seen in Fig. 14, not only was there no decrease in the energy dissipation capacity of the specimen after Point C despite all the damage, but the specimen also dissipated slightly more energy in the last cycle (i.e., Cycle 27) compared to Cycle 25. This demonstrates that the system is highly redundant with several load transfer paths, which helped the system to fulfill its function.

Conclusions

The behavior of PEC columns and the effect of the RBS connection on the behavior of the steel plate shear wall system were investigated in this experimental study. The main differences between this specimen and the benchmark specimen were the detailing of the columns, such as the use of reduced link spacings in critical regions and longitudinal rebars at the base, and use of RBS connections between the first-story beam and the columns. The reduced link spacing ($s/b = 0.2$) and the longitudinal rebars at the base of the columns, where plastic hinges were expected, improved the ductile performance of the column section significantly. The eventual formation of the plastic hinge at the top of the first-story column, resulting in a soft-story mechanism, was postponed because of the improvement of the column ductility at the base. The use of RBS frame connections improved the deformation mode of the system from flexural to shear by forcing the formation of plastic hinges at the ends of the first-story beam and reducing the rotational demands in the columns at the frame joints.

Considering the infill plate eventually detached from the south column along the weld line during the test, in order to ensure weld integrity complete inspection over the full weld length is necessary when thin infill plates are used. Alternatively, similar to the modular test (Dastfan and Driver 2016), fish plates thicker than the infill plate could be used to connect the infill plates to the surrounding beams and columns by bolting. The use of fish plates with bolted infill plate installation also facilitates the replacement of a damaged infill plate after the occurrence of an earthquake.

The initial stiffness of the test specimen was high, and the postpeak strength degradation was gradual. The displacement ductility of the specimen was 4.0 at the peak strength, and at 90% of the peak strength in the postpeak stage it was 6.2. The hysteretic loops of the specimen were stable and relatively wide, which led to a reliably high energy dissipation capacity in the plastic phase. Despite the complete tearing of the outer column flanges at the base and complete detachment of the infill plate from the south column in the first story, there was no sudden drop in the strength of the specimen, which indicates the high redundancy of the system. These observations verify that the specimen possessed the characteristics of an efficient lateral load resisting system during the service and extreme loading events.

Acknowledgments

Funding for this study was provided by the Natural Sciences and Engineering Research Council of Canada and the Canam Group. The first author received financial support in the form of scholarships from Alberta Innovates and the University of Alberta. Lehigh Inland Cement Limited provided the required concrete for this research.

References

AISC. (2010). "Seismic provisions for structural steel buildings." *ANSI/AISC 341-10*, Chicago.

ATC (Applied Technology Council). (1992). "Guidelines for cyclic seismic testing of components of steel structures." *Rep. 24*, Redwood City, CA.

Begum, M., Driver, R. G., and Elwi, A. E. (2007). "Finite-element modeling of partially encased composite columns using the dynamic explicit method." *J. Struct. Eng.*, 10.1061/(ASCE)0733-9445(2007)133:3(326), 326–334.

Bouchereau, R., and Toupin, J. D. (2003). "Étude du comportement en compression-flexion des poteaux mixtes partiellement enrobés." *Rep. EPM/CGS-2003-03*, École Polytechnique, Montreal (in French).

Chicoine, T., Massicotte, B., and Tremblay, R. (2002a). "Finite element modelling and design of partially encased composite columns." *Steel Compos. Struct.*, 2(3), 171–194.

Chicoine, T., Tremblay, R., Massicotte, B., Ricles, J., and Lu, L. W. (2002b). "Behaviour and strength of partially encased composite columns with built up shapes." *J. Struct. Eng.*, 10.1061/(ASCE)0733-9445(2002)128:3(279), 279–288.

CSA (Canadian Standards Association). (2014). "Design of steel structures." *CSA S16-14*, Mississauga, ON, Canada.

Dastfan, M., and Driver, R. G. (2008). "Flexural stiffness limits for frame members of steel plate shear wall systems." *Proc., 2008 Annual Stability Conf.*, Univ. of Missouri-Rolla, Rolla, MO, 321–334.

Dastfan, M., and Driver, R. G. (2009). "Investigations on the effect of frame member connection rigidity on the behavior of steel plate shear wall systems." *Proc., STESSA 2009 Behaviour of Steel Structures in Seismic Areas*, Taylor and Francis Group, London, 231–235.

Dastfan, M., and Driver, R. G. (2016). "Large-scale test of a modular steel plate shear wall with partially encased composite columns." *J. Struct. Eng.*, 10.1061/(ASCE)ST.1943-541X.0001424, 04015142.

Deng, X., Dastfan, M., and Driver, R. G. (2008). "Behaviour of steel plate shear walls with composite columns." *Proc., American Society of Civil Engineers Structures Congress*, ASCE, Reston, VA.

Deng, X., and Driver, R. G. (2007). "Steel plate shear walls with partially encased composite columns." *Proc., Structural Stability Research Council Annual Stability Conf.*, Univ. of Missouri-Rolla, Rolla, MO, 437–453.

Grubbs, K. V. (1997). "The effect of dogbone connection on the elastic stiffness of steel moment frames." M.Sc. thesis, Univ. of Texas at Austin, Austin, TX.

Moore, K. S., Malley, J. O., and Engelhardt, M. D. (1999). "Design of reduced beam section (RBS) moment frame connections." *Steel tips*, Structural Steel Educational Council, Moraga, CA.

Prickett, B. S., and Driver, R. G. (2006). "Behavior of partially encased composite columns made with high performance concrete." *Structural Engineering Rep. No. 262*, Univ. of Alberta, Edmonton, AB, Canada.

Qu, B., and Bruneau, M. (2010). "Capacity design of intermediate horizontal boundary elements of steel plate shear walls." *J. Struct. Eng.*, 10.1061/(ASCE)ST.1943-541X.0000167, 665–675.

Tremblay, R., Massicotte, B., Filion, I., and Maranda, R. (1998). "Experimental study on the behaviour of partially encased composite columns made with light welded H steel shapes under compressive axial loads." *Proc., 1998 Structural Stability Research Council Annual Technical Meeting*, Univ. of Florida, Gainesville, FL, 195–204.

Tremblay, R., Tirca, L., Bouchereau, R., Toupin, J. D., and Massicotte, B. (2003). "Flexural demand on partially-encased composite columns in multi-story concentrically braced steel frames." *Proc., STESSA 2003 Behavior of Steel Structures in Seismic Areas*, A.A. Balkema, Rotterdam, Netherlands, 479–485.

Vincent, R., and Tremblay, R. (2001). "An innovative partially encased composite column system for high-rise buildings." *Proc., North American Conf. on Steel Construction*, AISC, Chicago, 30-3–30-17.